

Evidence for cluster glass behavior in Fe₂VAl Heusler alloys

M. Vasundhara and V. Srinivas*

Department of Physics and Meteorology, Indian Institute of Technology, Kharagpur 721 302, India

V. V. Rao

Cryogenic Engineering Centre, Indian Institute of Technology, Kharagpur 721 302, India

(Received 26 December 2007; revised manuscript received 11 June 2008; published 4 August 2008)

Detailed magnetic measurements on intermetallic Fe₂VAl Heusler type alloys are presented. Annealed Fe₂VAl sample is structurally better ordered and exhibits higher magnetization, resistivity and magnetoresistance values compared to as cast samples. From the systematic analysis of magnetization and electrical transport data it has been established that the Fe₂VAl behaves more like a cluster glass. Magnetization as a function of magnetic field at various temperatures suggests the presence of superparamagnetic clusters along with paramagnetic background. Arrot plots confirm the absence of spontaneous magnetic moment and hence long-range ferromagnetic order down to 5 K. The field cooled and zero-field-cooled magnetization curves suggest the superparamagnetic entities freeze below 10 K. Our magnetoresistance data corroborate the magnetization results and confirm the presence of magnetic clusters.

DOI: [10.1103/PhysRevB.78.064401](https://doi.org/10.1103/PhysRevB.78.064401)

PACS number(s): 75.50.-y, 36.40.Cg, 72.15.Gd

I. INTRODUCTION

Although the study of electronic properties of Heusler-type intermetallic alloys has been actively pursued for more than three decades, there are still uncertainties in basic understanding of these materials. New and interesting results, theoretical as well as experimental, continue to appear even now. The renewed interest on these intermetallic alloys is triggered by the prediction of half metallicity of Heusler-type alloys by de Groot *et al.*¹ Half metallic materials share simultaneously the property of an energy gap between valence and conduction band electrons of one spin polarization and property of continuous band for the electrons of other spin polarization.¹⁻³ As a consequence, we have the remarkable situation that the conduction electrons at the Fermi energy (E_F) are 100% spin polarized and can result in unusual electronic properties that are suitable for spintronics applications. These systems are attractive from the both fundamental physics as well as industrial applications point of view as they exhibit a range of magnetic and electrical properties that show features reminiscent of magnetic semiconductors.

The ternary intermetallic Heusler alloys/compounds of stoichiometric composition with a general formula X_2YZ , where X and Y are generally represented by transition elements and Z a metalloid, exhibit a $L2_1$ crystal structure. Among various compositions, the Fe₂VAl Heusler alloy derived from substitution of V in place of Fe in a ferromagnetic Fe₃Al (DO₃ crystal structure) alloy, which exhibits remarkable magnetic and electrical properties.^{4,5} Although this alloy constitutes metallic elements it exhibits nonmetallic character, while it contains 50% of iron but reported to be nonmagnetic down to 2 K.⁴ These reports suggest that nonmetallic behavior is triggered by magnetic disorder in the Fe₂VAl compound. The observed large resistivity values and negative temperature coefficient of resistivity at low temperatures were attributed to a temperature dependent magnetic scattering. Further the magnetic and electrical transport properties of this composition are very sensitive to the substitution of elements and processing parameters.⁶⁻⁸ Matsushita and

Yamada⁶ found that the bulk properties of Fe₂VAl exhibit a very strong dependence on the heat treatment and subsequent cooling processes. They observed higher resistivity values for the quenched sample compared to the slowly cooled ones. The quenched materials, after heat treatment stage, exhibited semiconductorlike and nonmagnetic behaviors, while the slow cooled sample showed almost metallic transport and ferromagnetic transition. Maksimov *et al.*⁹ have also reported the existence of long-range ferromagnetic order below 13 K in slowly cooled Fe₂VAl through their microscopic magnetic measurements. They attributed the anomalous resistivity of nonmagnetic Fe₂VAl to the crystallographic disorder and chemical disorder, while the magnetic order to the presence of dilute magnetic ions in a nonmagnetic matrix. Further they rule out the proposition of generating magnetism through “Fe on the wrong (V) sites” can alone account for the magnetic order, as the number of wrong sited Fe are measured to be too low. On the other hand, from the magnetization and Mossbauer experiments it was suggested that the stoichiometric materials are nonmagnetic^{8,10} but contain antisite Fe atoms, which exhibit local magnetic moments or have superparamagnetic (SPM) clusters with at least two sizes and moments.^{7,10,11} These authors suggest that the SPM clusters form out of antisite disorder and the moments of Fe atoms in remaining disorder cells contribute to weakly magnetic state with no average moment. On the theoretical front, from first-principle calculations it has been shown that the Fe₂VAl in $L2_1$ structure has a nonmagnetic ground state and the magnetic moments if present are due to nonstoichiometry and antisite defects.¹²⁻¹⁵ These may be responsible for the large effective mass and the complex transport properties from low-density carriers interacting with localized magnetic moments.^{16,17}

On the basis of an extensive study on ternary Fe_{3-x}V_xAl alloy system, it has been suggested that the onset of ferromagnetism in these alloys is associated with a semiconductor to metal transition. Although semiconductor-metal-like transition has been demonstrated by several workers on substituting the elements such as Si (Ref. 18) and Ge (Ref. 19) in

place of Al, the interrelation between the magnetic and electrical transport properties has not been established in these systems. For example, a wide range of unusual properties such as high values of electrical resistivity (ρ), Seebeck coefficient,^{18–20} giant magnetoresistance,²¹ and extraordinary Hall effect²² have been reported by fine tuning the composition and process parameters. Therefore, we believe this composition is a suitable candidate for the multifunctional applications and hence it is essential to understand the physics underlying these peculiar but useful properties. On the other hand, magnetoresistance (MR) is intrinsically connected with the electron mean-free path, i.e., with a range of distances of the order of a few nanometers. The large MR values observed in magnetically heterogeneous media are satisfactorily explained on the basis of the spin dependent scattering of the electrons.²³ For example, the magnetization and magnetic transport properties of granular alloys (consisting superparamagnetic particles embedded into metallic nonmagnetic matrix) have been extensively studied.^{23–25} A natural extension provided by magnetic system in which magnetic inhomogeneity on nanometric scale is no longer related to chemical effects and comes instead from magnetic frustration effects originated by competing magnetic interactions. In such systems simultaneous presence of nonsaturating magnetization behavior up to very large field and huge steep magnetization changes at lower fields as well as evidence for irreversible effects are seen in the past.^{26–32} Since magnetization and magnetotransport measurements provide complementary information, one can obtain an unambiguous picture about the magnetic ground state of the sample in question. The magnetization and electrical transport behaviors of Fe_2VAl have been investigated under the influence of external magnetic field in the literature by different groups. These results have been explained by assuming the presence of magnetic clusters that have a metallic nature in the nonmetallic Fe_2VAl .^{6,22} We believe that a comparative study of magnetic and magnetotransport properties on Fe_2VAl for which process conditions and methods of preparation are the same, can provide information on the magnetic ground state of the sample.

In this work, we intend to present an in-depth study on thermal and external magnetic-field dependences of magnetization and electrical transport behaviors of Fe_2VAl alloys synthesized under similar processing conditions. Significant differences in magnetic and magnetoresistance values have been observed and related to the magnetic disorder. The question that needs to be addressed here is whether the magnetic transition observed at low temperatures (in most of the magnetic studies reported so far) is ferromagneticlike or glassy-state-like. By performing detailed analysis of the above data we show that the presence of magnetic clusters (superparamagnetic, ferromagnetic) plays a significant role in altering the magnetic and magnetotransport behaviors.

II. EXPERIMENT

The alloy ingots of Fe_2VAl were prepared by arc melting with high-purity elemental constituents under argon atmosphere. Then ingots were annealed in evacuated quartz ampoules at 1200 K for 48 h. Both the as cast and annealed

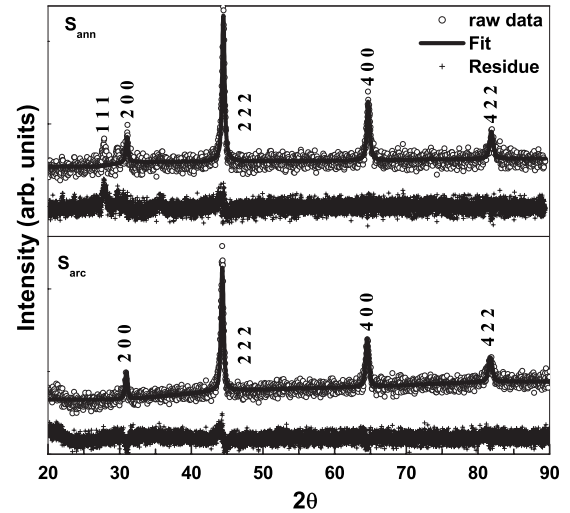


FIG. 1. XRD patterns of Fe_2VAl alloys (S_{arc} and S_{ann}) along with fits to the data.

samples were then cut into suitable shapes for the physical property measurements. Remaining part of the ingots was used for the structural investigations. Since present work deals with the experimental results on a single Fe_2VAl composition, we represent the arc-melted sample as S_{arc} and the sample that is slowly cooled after annealing is referred as S_{ann} in the following description. The crystallographic structure is identified by x-ray diffraction (XRD) using a P.W. 1718 x-ray diffractometer with filtered $\text{Cu } K_\alpha$ radiation of wavelength $\lambda=0.15418$ nm. Nominal composition assigned to each sample was regarded as accurate because the weight loss was found to be less than 0.3–0.5%. Further the elemental analysis was done using an energy dispersive x-ray analyzer attached with field-emission scanning electron microscope (FESEM) (Carl Zeiss, Supra 40). The surface microstructure measurements and elemental analysis was carried out at several locations on well-polished surfaces of the sample. The average composition of the sample is estimated to be $\text{Fe}_{2.03}\text{V}_{1.01}\text{Al}_{0.96}$, which is in the vicinity of Fe_2VAl composition. The analytical values are quite consistent with the nominal composition reported in this study. Magnetization data as a function of applied fields up to 50 kOe and temperatures down to 5 K were taken using a commercial superconducting quantum interference device (Quantum Design) magnetometer. Electrical resistance measurements as a function of temperature (5–300 K) and applied magnetic field (0–50 kOe) have been carried out using conventional four-probe technique in a cryogen-free superconducting magnet system.

III. RESULTS AND ANALYSIS

A. X-ray diffraction

As cast (S_{arc}) and annealed (S_{ann}) samples of Fe_2VAl alloy do not show significant differences in x-ray diffraction patterns shown in Fig. 1. The presences of strong reflections at (200), (220), (400), and (422) in XRD patterns confirm the $L2_1$ crystal structure. However, on close examination of

TABLE I. Comparative physical parameters of as-cast and annealed Fe₂VAl samples. Resistivity values at 300 K ($\rho_{300\text{ K}}$), 5 K ($\rho_{5\text{ K}}$) temperature; magnetization values at 5 K ($M_{5\text{ K}}$), a is lattice constant, and $\Delta R/R_{5\text{ K}}(\%)$ is magnetoresistance percent in 50 kOe field at 5 K.

Sample	$\rho_{300\text{ K}}$ (m Ω Cm)	$\rho_{5\text{ K}}$ (m Ω Cm)	$M_{5\text{ K}}$ (emu/g) (50 kOe)	a (\AA)	$\Delta R/R_{5\text{ K}}(\%)$ (50 kOe)
As-cast (S_{arc})	1.358	4.288	2.70	5.774	-8.32
Annealed (S_{ann})	1.512	5.020	4.23	5.761	-9.80

XRD pattern of the S_{ann} sample one can observe a weak (111) peak, while this is not discernible in the case of S_{arc} sample. These features are attributed to certain site interchanges and structural disorder. Annealing and subsequent slow cooling result in formation of better-ordered phase than that of quenched samples of Fe₂VAl. Detailed analysis of the x-ray diffraction data was performed with the Reitveld structural analysis using FULL PROOF 2K (version 3.4) program. As shown in Fig. 1, from the residues one can judge the quality of the fits to data to be good. The analysis shows a cubic structure that can be identified by $Fm\bar{3}m$ space group for both the S_{ann} and S_{arc} samples. The lattice parameters thus obtained are shown in Table I. The lattice parameter obtained from the analysis for S_{ann} is in agreement with the earlier reported value^{4,5} while S_{arc} shows larger values compared to the annealed samples indicating lattice strain.

The physical properties of Fe₂VAl alloy are sensitive to the structure and composition; minute structural changes observed in XRD patterns also reflect in magnetic and electrical properties. As shown in Table I, S_{ann} samples show higher values of electrical resistivity and magnetization (M) compared to S_{arc} alloys. In contrast, Matsushita and Yamada⁶ have reported higher resistivity values at low temperature for quenched samples than that of slow cooled ones, while the magnetization data exhibit a similar trend observed in the present study. On the other hand, a long-range ferromagnetic order below 13 K has been reported in slowly cooled Fe₂VAl composition through microscopic magnetic measurements.⁹ Our results are in deviation with the earlier reports,^{6,9} but show similar trend to those reported by others.⁷ A systematic magnetic and electrical transport investigations on the samples having compositions in the vicinity of Fe₂VAl revealed a direct relation between electrical resistivity and magnetic moment of Fe₂VAl system,³³ which is consistent with the data given in Table I. Since the electrical and magnetic properties are very sensitive to the impurity and disorder the physical properties can also be used for assessing the quality of the sample.^{33,34} Although the composition analysis shows minute deviations from the 2:1:1 composition, the magnitudes of resistivity and magnetization values of S_{ann} are similar to the one reported in the literature confirming the superior quality of the sample.^{4,7} Therefore, a detailed investigation of magnetic properties has been carried out in order to understand the thermal evolution of magnetic and related electrical transport behaviors of this composition. Further a comparative study of S_{ann} and S_{arc} can provide evidence on how the disorder or defects alter the properties of the material.

B. Thermal variation of magnetization

The zero-field-cooled (ZFC) and field-cooled (FC) magnetization curves as a function of temperature under the external field of 100 Oe is shown in Fig. 2 for S_{arc} and S_{ann} samples. The magnetization data measured as a function of

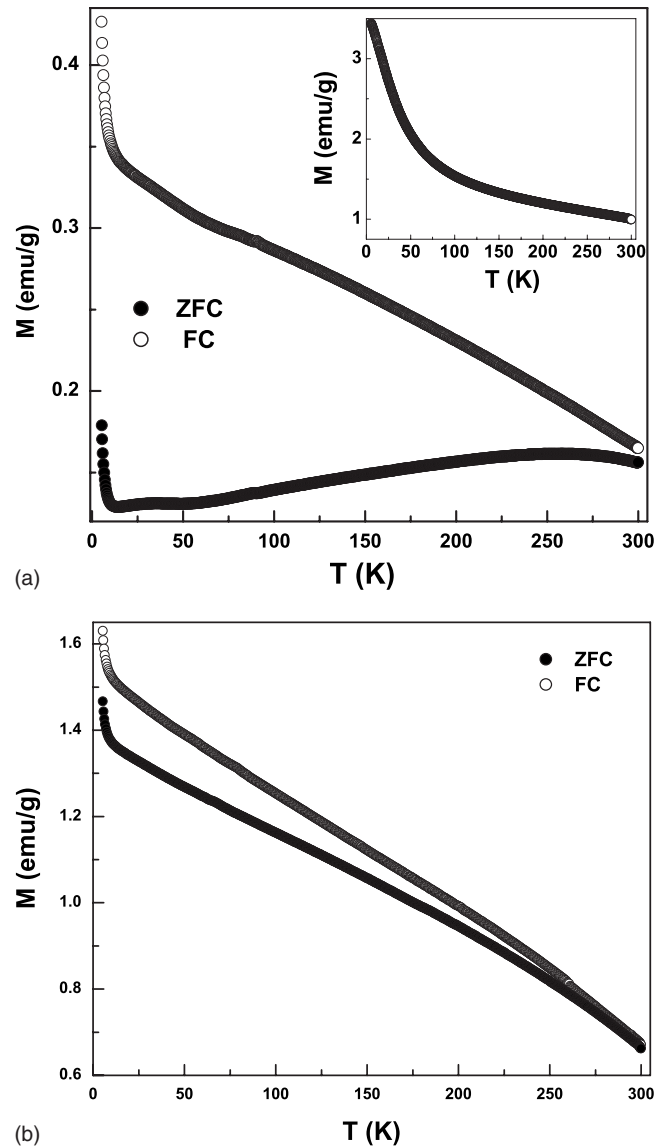


FIG. 2. FC and ZFC curves of Fe₂VAl at $H=100$ Oe for (a) S_{arc} alloy; Inset: Temperature variation of magnetization under applied field of 90 kOe (b) S_{ann} alloy.

temperature show some interesting features: (i) as the temperature is lowered from 300 K the ZFC magnetization curve of S_{arc} sample shows an increase in M down to 260 K and then decreases down to 11 K, below which a rapid increase in M is observed, while for FC curve M increases as the temperature is lowered and with an abrupt increase in M below 11 K; (ii) irreversibility in ZFC and FC curves is observed from 300 K; (iii) when the sample is cooled in 90 kOe applied field the magnetization process appears to be modified, in the sense, a sharp increase in M was not observed; (iv) as the temperature is lowered the ZFC and FC curves of S_{ann} sample show rise in magnetization with a sharp increase in M at lower temperature (10 K), but the irreversibility in FC and ZFC curves occurs below 250 K; (v) the magnetization values of S_{ann} are higher than that of S_{arc} sample. We define the temperature of irreversibility T_{irr} as temperature at which the FC and ZFC curves begin to diverge. Lower magnetization values and irreversibility of $M(T)$ curves on application of small magnetic fields suggest the presence of magnetic disorder in the samples. In general, T_{irr} along with a peak in the ZFC curves has been reported in the systems that possess mixed exchange interactions, such as spin glass or magnetic clusters.²³⁻²⁵ In these systems the moments interact with one another via the magnetic-dipole interactions, $J_{ij} = \mu_i \mu_j (1 - 3 \cos^2 \theta_{ij}) / r^3$. The large μ_i moves the characteristic interaction from the millikelvin to kelvin temperature range. This interaction can be either FM or AFM depending on the relative orientation of each dipole. Thus a disordered dipolar system can behave as a cluster glass. Although band-structure calculations suggest that Fe_2VAl is nonmagnetic,¹³⁻¹⁵ there have been some reports which show evidence of superparamagnetic state^{6-8,10,11,22} with varying freezing temperature values, while other microscopic magnetic measurements suggest a FM order at low temperature.⁹ Present observations along with earlier reports suggest that the S_{arc} sample is magnetically disordered and the broad features of ZFC curves suggest the presence of distribution of magnetic clusters/defects, manifested through the large T_{irr} and a broad maximum in ZFC curves. Superparamagnetic systems also exhibit a divergence in FC/ZFC curves below the blocking temperature, but the nature of these curves depends on various magnetic parameters such as magnetic anisotropy, interparticle interactions, etc. The $M(T)$ curves under an applied field of 90 kOe neither show a sharp raise at lower temperatures nor follow a Curie-Weiss behavior. However, present results suggest that the system comprises of two-magnetic components (presumably a weakly ferromagnetic at low temperature and other (super)para- or antiferromagnetic entity). A magnetic ordering temperature in the form of sharp rise in $M(T)$ is observed in the vicinity of 11 K, which is consistent with earlier reports.⁷ Since this abrupt increase is observed in both S_{arc} and S_{ann} (ZFC and FC curves), we believe that these clusters freeze (with magnetization in random directions) below 11 K. Further it is clear from the FC curves that the clusters cannot be aligned even in the presence 100 Oe magnetic field. From T_{irr} we can suggest that S_{ann} sample has narrow size distribution of clusters compared to S_{arc} . In order to obtain a deeper understanding we have carried out isothermal magnetization measurements on S_{arc} sample over the temperature range 5–300 K.

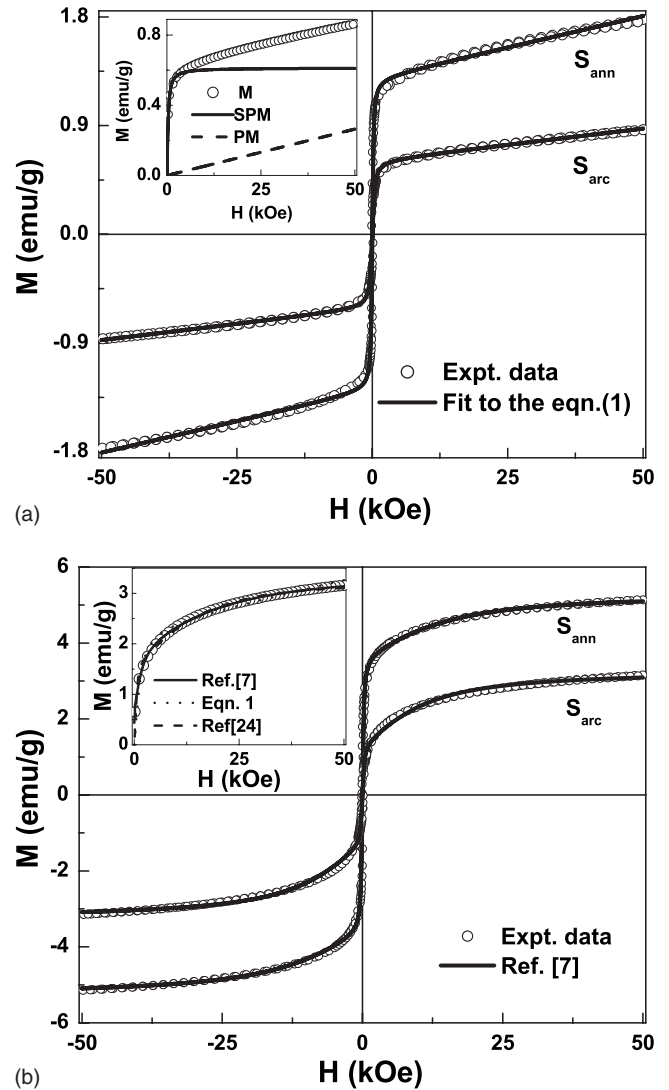


FIG. 3. M - H plots of S_{arc} and S_{ann} alloys (a) at room temperature along with the fits (solid lines) to Eq. (1). Inset shows separated components of S_{arc} alloy. (b) At 5 K along with the fits (solid lines) to the two-cluster model. Inset shows M - H curve of S_{ann} sample along with the fits to Eq. (1) and models of Refs. 7 and 24.

C. Magnetic-field dependence of magnetization

The magnetization data as a function of applied field (H) has been recorded for S_{arc} and S_{ann} samples at 300 and 5 K. Typical isotherms for both these samples are shown in Figs. 3(a) and 3(b). The curves at 300 K display low magnetization values along with rapid increase in magnetization at low magnetic fields but do not saturate even at applied magnetic fields of 50 kOe. On the other hand 5 K magnetization data show a significant increase in magnitude along with a tendency to saturate at higher applied fields. This unusual behavior can be due to the presence of two-magnetic components, i.e., a ferromagnetic (FM) component that is easily saturated at low fields and a linear component with large high-field susceptibility could be considered SPM or paramagnetic (PM). In order to investigate whether the sharp rise in M vs H curves at low field is due to interaction effects or FM component, hysteresis loops were recorded at various

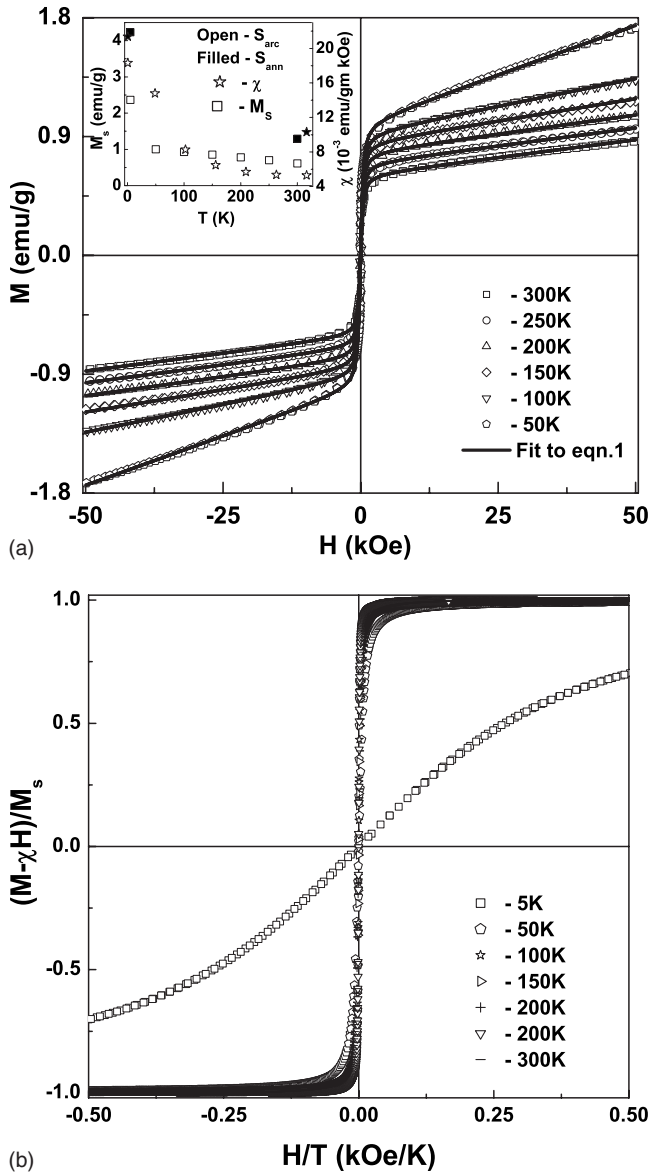


FIG. 4. (a) M - H plots of S_{arc} alloy at different temperatures along with the fits to Eq. (1). Inset: Saturation magnetization and susceptibility obtained from the fits vs temperature. (b) A plot of $(M - \chi H)/M_s$ vs H/T at different temperatures.

temperatures between 5 and 300 K. As shown in Figs. 3 and 4(a) the small area of measured loop and the slow approach to the saturation are good indications of the presence of a SPM phase. The presence of FM behavior is however, evidenced by the remanence magnetization and sharp increase in M at low fields. It is also important to note that the saturation of the magnetization is not reached even for applied magnetic fields as large as 50 kOe. Further, magnetization values increase on annealing but no significant change in coercivity (H_C) is observed. Further a strong support in favor of the nonexistence of long-range ferromagnetic Fe state stems from the Mossbauer spectra analysis, in which no significant hyperfine field has been observed and attributed to the presence of magnetic clusters with weak Fe-site moments in this system.^{10,26} These results indicate that the FM component possibly stems from the strong intercluster interac-

tions or distribution of cluster sizes with varying magnetic properties.

Presently there exists no unified model which can describe the combined FM and SPM magnetization curves generally obtained in complex magnetic systems. Consequently, we have adopted the empirical approach and analyzed each magnetization curve as a sum of two contributions: a FM +PM, FM+SPM, or SPM+PM. Among various combinations of magnetic contributions, SPM and PM combinations follow the experimental data quite well with the minimum number of fit parameters resulting in a best least square fit. A modified Langevin function represented by

$$M(H) = M_s L(\mu H/kT) + \chi H \quad (1)$$

is used to fit the $M(H)$ data above 10 kOe. Here μ is the average magnetic moment per particle, $L(x) = \cos(x) - 1/x$ is the Langevin function, M_s is the saturation magnetization, and χ is the susceptibility. The solid lines through the data points in Figs. 3 and 4 are fits to Eq. (1). Typical PM and SPM components are shown in the inset of Fig. 3(a) for 300 K data. The other combinations such as FM, SPM, and FM, PM contributions did not yield good fits to the experimental data suggesting that the more likely magnetic nature of the grains is SPM. On the other hand the Eq. (1) did not yield good fits to 5 K M vs H curves. However, the two cluster model fits⁷ yielded reasonably good fits to the data as shown in the inset of Fig. 3(b) with cluster magnetic moments to be $535\mu_B$ and $15\mu_B$ for S_{arc} and $710\mu_B$ and $10\mu_B$ for S_{ann} , respectively. We have also attempted to fit the data to a combination of terms representing FM and SPM models following Ref. 24 that yielded good fits to the data and will be discussed later. We have obtained good fits with two-cluster model, but this could be argued as due to extra free parameter used in the equation. Further these fits result in larger cluster moments as the temperature is increased, which is difficult to explain by simple superparamagnetic cluster model. Strong increase in M and χ [see inset of Fig. 4(a)] as the temperature is decreased could be attributed to enhanced dipole interactions between the clusters that probably give rise to a FM-like magnetization characteristics. However, in spite of these interactions and anisotropy, it is possible to extract an average size of the magnetic particles from the high-field behavior of magnetization. Reasonably good fits were obtained for all the magnetic isotherms with two component model, i.e., Eq. (1) except for 5 K data. This analysis indicates the presence of magnetic clusters in a PM matrix and enhanced intercluster interaction at lower temperatures.

To ascertain a superparamagnetic state in a material one needs to satisfy the two basic requirements, namely, (i) the magnetization curve must show no hysteresis since that is not a thermal equilibrium property, and (ii) the magnetization curve for an isotropic sample must be temperature dependent to the extent that curves taken at different temperatures must approximately superimpose when plotted against H/T after correction for the temperature dependence of the spontaneous magnetization. However, this behavior is quite different from that usually observed for very small ferro- and ferrimagnetic particles. All the normalized isotherms that were plotted against H/T do not follow an universal curve and

deviations have been observed in the higher field region. This is anticipated, as the data do not follow a simple Langevin function that is expected for the superparamagnetic samples. However, all the isotherms above the temperature 50 K fit to a functional form given in Eq. (1). Therefore, by subtracting the linear component and normalizing with M_s , $[(M-\chi H)/M_s]$ vs H/T data are replotted in Fig. 4(b). As shown in the figure all the isotherms $T \geq 50$ K collapse on a single universal curve. These results further support the viewpoint that SPM component exists in the temperature range 50–300 K along with a PM or AFM (to account for high-field linear M) component. However, a strong deviation from this behavior has been observed when 5 K data were also plotted on the same graph. This could be due to the development of higher magnetization state below temperatures $T \sim 10$ K (see Fig. 2), where a sharp increase in magnetization has been observed in FC and ZFC curves. Further this is consistent with the observation that the $M(H)$ data at $T=5$ K (i) do not yield a good fit to Eq. (1) and (ii) a saturation tendency is seen at higher applied magnetic fields. These results suggest that the magnetic transition observed below 50 K could be due to the blocking of SPM cluster. However, on application of magnetic field these clusters can align easily in the direction of external magnetic field and result in saturation tendency of the magnetization curve below 10 K. However, the question now remains to be answered is whether the sample exhibits long-range ferromagnetic order at 5 K or not. In order to examine this we have attempted to estimate the spontaneous magnetization of the sample.

Figure 5 shows an Arrot plot of the $M(H)$ data for $H \leq 50$ kOe and $5 \text{ K} \leq T \leq 300 \text{ K}$. The features that are of interest in this figure can be summarized as follows: (i) The Arrot plots are not linear, unlike those for ferromagnetic (even weak ferromagnet) materials at any given temperature. Therefore, this rules out the possibility of PM to FM transition in this temperature interval. (ii) A strong curvature toward the H/M axis beginning at moderate fields (~ 7 kOe). (iii) No evidence of spontaneous magnetization at any temperature (no intercept on M^2 axis). However, extrapolating from high fields produce an intercept, which indicates a field-induced FM alignment of the moments. The strong curvature at low fields and general shape of the Arrot plot is reminiscent of the behavior theoretically predicted by Aharony and Pytte²⁷ (AP) of a random anisotropy system with weak anisotropy. AP predicted a transition from PM to an infinite susceptibility phase with no long-range magnetic order in zero fields. If higher-order anisotropy terms are considered, the susceptibility is large but finite, i.e., the intercept on H/M axis is small, but nonzero. The data in figure exhibit behavior very similar to the AP prediction that has been invoked for the interpretation of experimental results for the amorphous alloys having strong and weak anisotropies. A change in curvature in Arrot plots is not unique to amorphous FM, it also occurs in dipolar systems with random anisotropy. Another important fact is the absence of spontaneous magnetization, which implies that the FM-like behavior below 10 K is spatially confined, i.e., only clusters of FM order exist. This is in agreement with earlier conclusion that the SPM particles get blocked in a FM cluster state. This

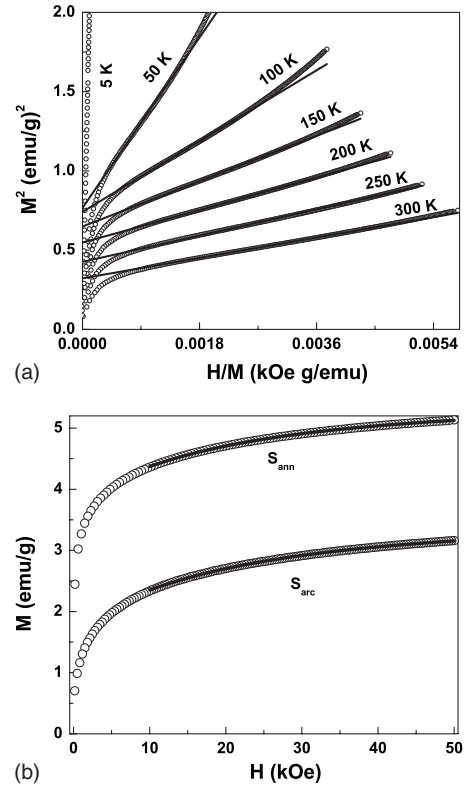


FIG. 5. (a) Arrot plots at different temperatures of S_{arc} sample. (b) M - H plots of S_{arc} and S_{ann} alloys at 5 K and solid lines represent fits to Eq. (3) (see the text).

observation is in agreement with the results obtained from the Mossbauer experiments.^{10,26}

Chudnosky *et al.*²⁸ have developed a theory of ferromagnetic materials having random anisotropy that has led to different kind of magnetic ground states, depending on the strength of the field. The strength of H is measured relative to a parameter H_s , where $H_s = H_r^4 / H_{\text{ex}}^3$. H_r is the anisotropic field and H_{ex} is the exchange field. For low fields $H < H_s$ one has a correlated spin glass, which has a large susceptibility and is equivalent to the AP high-susceptibility phase. The random anisotropy causes the directions of the magnetization of locally correlated regions to vary. This regime is called the ferromagnet with wandering axis. In this regime, the magnetization approaches saturation as

$$M = M_0 \left[1 - \frac{1}{15} \left(\frac{H_s}{H} \right)^{1/2} \right], \quad (2)$$

where M_0 is the saturation magnetization. For high fields $H > H_{\text{ex}}$, all spins are virtually aligned with the field and there is only a slight tipping angle due to the anisotropy. In this regime, M is predicted to approach M_0 as

$$M = M_0 \left[1 - \frac{1}{15} \left(\frac{H_r}{H + H_{\text{ex}}} \right)^2 \right]. \quad (3)$$

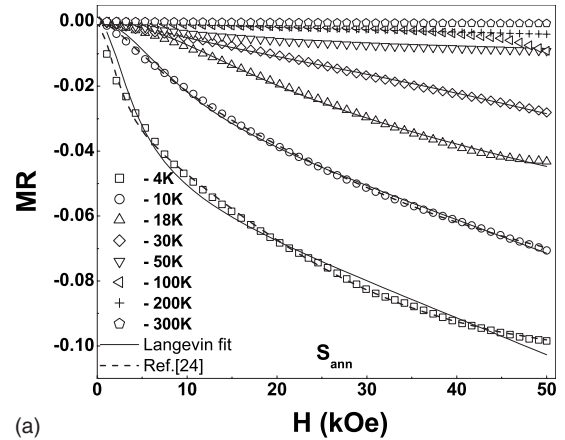
In Fig. 5(b), a graph of M vs H for $10 \leq H \leq 50$ kOe at 5 K is shown, along with a fit to Eq. (3), which agrees well with the experimental data. The fit parameters extracted from both as cast and annealed samples are $M_0 = 3.54$ emu/g,

$H_r=119$ kOe, and $H_{ex}=43$ kOe and $M_o=5.47$ emu/g, $H_r=88$ kOe, and $H_{ex}=41$ kOe, respectively. From these fits it is clear that anisotropic field is much smaller in annealed samples. For validity of Eq. (3) a requirement $H > H_{ex}$ has been met by present fits. Relatively high level of anisotropy that seems to characterize this system suggests that the low-temperature state of the anisotropy is strongest. More likely the situation is that there are FM correlated regions, the sizes of which are limited by the grain sizes whose magnetization directions are pinned or frozen by random anisotropy. In other words at lower temperatures where the strength of the random anisotropy is higher the magnetization of correlated regions freeze into a cluster glass state.

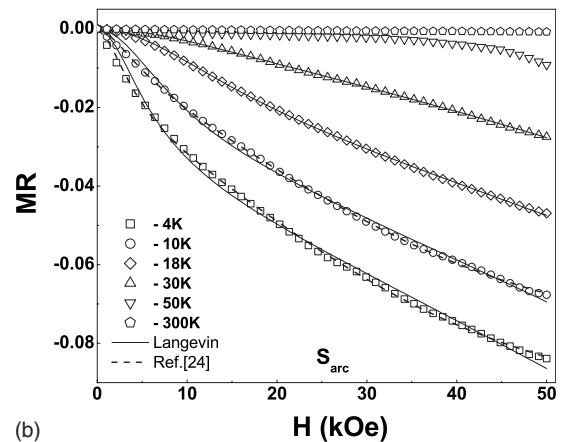
D. Magnetic-field dependence of resistance

Absence of spontaneous magnetization is suggestive of lack of long-range magnetic order, while sharp increase in magnetization at lower field and a nonsaturation magnetization behavior up to higher field indicate the presence of short-range magnetic correlations. On the other hand, observation of negative temperature coefficient of resistivity with large values of resistivity at a composition near where long-range magnetic order breaks down is the feature that indicates the existence of some correlation between magnetic and electrical properties. Further on annealing S_{arc} sample both magnetization and electrical resistivity values increase (see Table I), which is contrary to the reported values reported by earlier groups. Therefore, magnetoresistance measurements on the samples have been carried out. The important parameter that determines the resistance variation with field is $\langle \cos \varphi_{ij} \rangle$, where φ_{ij} is the angle between the axes of ferromagnetic entities over a distance of electronic mean-free path. For noninteracting particles if magnetization vectors are uncorrelated, the MR follows a quadratic dependence of reduced magnetization.²⁹ Any deviation from this law is indicative of the existence of correlations and therefore interaction effects between neighboring particles should be taken in to account.³⁰ Recently, a significant giant magnetoresistance effect has been observed in the paramagnetic phase of the homogeneous $Au_{80}Fe_{20}$ alloys.^{25,31} Another important parameter in obtaining higher MR values is the magnetic particle size, which directly determines the spin-dependent scattering through the surface-to-volume ratio and particle distance. The model predictions agree with experiments, where an inverse proportionality between the magnetic cluster size and the MR ratio has been generally observed.

Figure 6 shows MR as a function of H for S_{arc} and S_{ann} samples at different temperatures. The MR calculated in the present investigation is defined as $\Delta\rho/\rho = [\rho(H, T) - \rho(0, T)]/\rho(0, T)$, where $\rho(H, T)$ is the resistance of the sample in magnetic field at a temperature. The electrical resistivity (ρ), MR, and magnetization values at a particular applied magnetic field are higher for annealed samples compared to as-prepared samples. This observation along with $M(T)$ curves (ZFC, FC) suggest that the as-prepared samples are disordered (distribution of magnetic clusters) compared to annealed ones. In all cases it is seen that $\Delta\rho/\rho$ is negative and MR values decrease as the temperature is increased,



(a)



(b)

FIG. 6. MR vs H at different temperatures along with the Rubenstein (Ref. 24) and Langevin fits.

which is in agreement with earlier reports.²¹ The MR is far from saturation even in 50 kOe, which indicates an important contribution of spin disorder to the MR. A similar MR behavior has been reported in granular CoCu (Refs. 23–25) cluster glass AuFe alloys.³² From the present magnetization, MR data along with Mossbauer and NMR measurements in the literature suggest an existence of magnetic clusters in these alloys. However, deviation from quadratic dependence of $\Delta\rho/\rho$ on M_s could be due to the existence of magnetic interactions among the clusters or to the large particle size distribution with magnetic characteristics from FM to spin-glass range. Our magnetization data suggest the coexistence of FM and PM/SPM clusters in the samples. In order to account for these characteristics we have attempted a fit to MR data through a phenomenological model with a combination of SPM, PM or FM, SPM entities oriented in random fashion. Therefore, the field dependent MR is expressed as an even function of the reduced magnetization $m = M(H)/M_s$, $M(H)$ is global magnetization and M_s is the saturation value

$$\frac{\Delta\rho}{\rho} = -\alpha F(m),$$

where $F(m)$ is an even function of m and prefactor α sets the overall magnitude of the MR. The function $F(m)$ was tried

with combination of FM and PM terms as implemented by Rubinstein *et al.*²⁴ An attempt is also made to fit the data assuming the $F(m)$ to be Langevin function, which was used to fit the magnetization data. The low-temperature MR data of as-prepared and annealed samples along with the fits to the above schemes are presented in Fig. 6. It is clear from the figure that the Langevin model did not yield good fits to the MR data at 5 K, which is similar to the case of $M(H)$ curves. However, a combination of FM and PM (Ref. 24) cluster model seem to yield reasonably good fits, establishing the fact that the Fe_2VAl samples contain a distribution of cluster sizes ranging from SPM to FM. These conclusions are supported by the magnetization results discussed earlier.

IV. DISCUSSION

Intermetallic compound Fe_3Al is a ferromagnetic having Curie temperature (T_C) ~ 770 K with a Do_3 crystal structure. The Fe_2VAl composition is derived from the Fe_3Al by substituting “V” in place of “Fe.” It is observed that the T_C and magnetic moment decrease with increasing V concentration and long-range FM order disappears in the vicinity of Fe_2VAl composition. Although S_{ann} and S_{arc} samples exhibit similar XRD patterns and lattice parameters, significant differences in magnetic and electrical properties have been observed. The S_{ann} sample exhibits higher magnetization and resistivity (ρ) values compared to S_{arc} . The higher ρ values in S_{ann} suggest that the ground (ordered) state is nonmetallic in nature. Enhanced magnetization values in S_{ann} suggest that this is the intrinsic property of the Fe_2VAl sample in which either a crystallographic superstructure exists¹² or more Fe/V site exchanges are present.^{13–15} Magnetization as a function of temperature (ZFC, FC) suggests the presence of a magnetic disorder and a transition in the vicinity of 10 K. When the sample is cooled in 90 kOe field the larger clusters get aligned at 300 K and subsequent temperature dependence is PM-like. This also confirms the bimodal cluster distributions. Absence of spontaneous magnetization even below 11 K (Arrot plots) together with the existence of at least two-magnetic components in M vs H curves suggest the presence of magnetic clusters without any long-range ferromagnetic order. Further analysis of M vs H curves at different temperatures shows that the long-range magnetic order is destroyed although a gamut of large FM clusters is still present indicating a cluster glass or SPM state with interaction effects. Here the cluster glass phase develops from FM (Fe_3Al) state possibly due to the random anisotropy (dipolar) due to the presence of V.¹⁰ It is observed that on substitution of early transition metals (ETM) such as Cr, V, and Mn in Fe-rich alloys, the T_C and magnetic moment (μ) decrease with increasing concentration of ETM. This is attributed to the AFM coupling between the Fe and the early transition metals. In some cases such as Fe-based amorphous alloys when Cr or Mn substituted for Fe, it is observed that the system transforms to a more frustrated system due to the coexistence of FM and AFM regions in the sample.³² These systems exhibit a variety of magnetic characteristics such as re-entrant spin glass, cluster glass, or micromagnetic behavior. Various suggestions have been proposed for such systems, one of which is

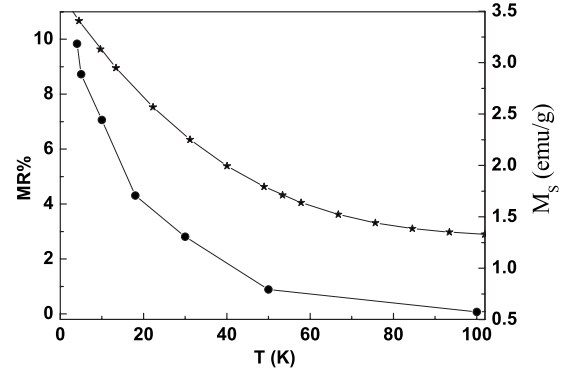


FIG. 7. Magnetization and MR% as a function of temperature in applied magnetic field of 50 kOe.

the appearance of temperature dependent anisotropy. At low temperatures this anisotropy grows sufficiently large that severs many of the weak links holding together the rather tenacious infinite clusters. Then the anisotropy points these divided clusters along the randomly preferred directions. However, the “infinite cluster” FM state is not truly long ranged. Instead, it consists of many extremely large clusters, which are hard to tell from infinite. These large, but disordered from each other, clusters then dissociate into the collection of smaller clusters at lower temperatures. Such processes occur within the usual percolation phase transition.

When the magnetic behavior is dominated by the presence of large magnetic clusters, the term cluster glass used and some of these clusters embedded in weakly magnetic matrix. At sufficiently low temperatures, these clusters freeze with random orientation in a manner analogous to spin-glass freezing. The cluster glasses are especially sensitive to their metallurgical state, i.e., heat treatment, with various times, temperatures, and cooling rates, along with plastic deformation can greatly affect the cluster formation and in turn magnetic behavior. As discussed earlier, presently investigated samples exhibit such features and from this we suggest that the magnetic ground state of the Fe_2VAl belongs to cluster glass state. The origin of these clusters with different magnetic moments is believed to be due to the site occupancy in crystal structure that has been confirmed by earlier theoretical studies and experimental observations. Using bimodal distribution of magnetic clusters large MR can also be consistently explained, i.e., the moments of large particles will be more easily aligned than smaller ones at a given temperature. The large clusters are then responsible for the low-field variation of the MR and small ones for the slow approach. Therefore, the variation of MR is dictated by the cluster sizes. The presence of the magnetic clusters originates from some disorders between Fe and V atoms. As shown in Fig. 7 the MR and M (obtained from Arrot plots) follow same trend indicating an existence of correlations between the cluster sizes and interactions among them to the MR behavior. The strong increase of MR with decreasing temperature is due to the increased tendency of alignment of the moments of the granules in the external field. Nishino *et al.*³³ recently demonstrated a similar interrelation between magnetic and electrical properties where they showed that the electrical resistivity is directly proportional to the average magnetic

moment of Fe atoms. These observations are in good agreement with theoretical calculations^{14,15} that predict varying local moments from different site disorders.

V. CONCLUSIONS

We have reported a comprehensive study of magnetic and magnetoresistance results on as cast and annealed Fe₂VAl alloys. Although significant changes were not observed in the XRD patterns the magnetic and magnetoresistive properties show significant changes. The magnetization data support the presence of superparamagnetic clusters through expected scaling of the normalized magnetization vs H/T curves. Arrot plot clearly shows nonexistence of transition temperature and spontaneous magnetization in the temperature range 50–300 K, but an abrupt increase in magnetization below 10 K suggests the freezing of clusters. Both magnetization as well as magnetoresistance show similar changes at low tempera-

ture, suggesting the formation of more ordered clusters which result in large MR values that is reminiscent of granular alloys. From a detailed analysis of bulk magnetization data, we rule out the possibility of FM state at low temperatures. Instead it is observed that samples contain magnetic clusters of different sizes. All these observations unequivocally establish the ground state of the Fe₂VAl to be a cluster glass, having magnetic clusters of different sizes.

ACKNOWLEDGMENTS

The present work is partially supported by the Board of Research in Nuclear Sciences (BRNS), Department of Atomic Energy (DAE), Mumbai, India. The financial assistance provided to one of the authors (M.V.) by the Council of Scientific and Industrial Research (CSIR), India, is gratefully acknowledged. The authors also would like to acknowledge FIST and Nanoinitiative programs of DST for low-temperature MR and FESEM data.

*Corresponding author. FAX: +91-3222-255303. veeturi@phy.iitkgp.ernet.in

¹R. A. de Groot, F. M. Mueller, P. G. van Engen, and K. H. J. Buschow, Phys. Rev. Lett. **50**, 2024 (1983); R. A. de Groot and K. H. J. Buschow, J. Magn. Magn. Mater. **54-57**, 1377 (1986).

²W. E. Pickett and J. S. Moodera, Phys. Today **54** (5), 39 (2001).

³I. Zutic, J. Fabian, and S. Das Sharma, Rev. Mod. Phys. **76**, 323 (2004).

⁴Y. Nishino, M. Kato, S. Asano, K. Soda, M. Hayasaki, and U. Mizutani, Phys. Rev. Lett. **79**, 1909 (1997); Y. Nishino, Shin-ya Inoue, S. Asano, and N. Kawamiya, Phys. Rev. B **48**, 13607 (1993).

⁵Y. Nishino, C. Kumada, and S. Asano, Scr. Mater. **36**, 461 (1997); Y. Nishino, M. Matsuo, S. Asano, and N. Kawamiya, Scr. Metall. Mater. **25**, 2291 (1991).

⁶A. Matsushita and Y. Yamada, J. Magn. Magn. Mater. **196-197**, 669 (1999); A. Matsushita, T. Naka, H. Mamiya, Y. Takano, T. C. Ozawa, K. Fukuda, and Y. Yamada, *ibid.* **272-276**, 783 (2004).

⁷Ye Feng, J. Y. Rhee, T. A. Wiener, D. W. Lynch, B. E. Hubbard, A. J. Sievers, D. L. Schlagel, T. A. Lograsso, and L. L. Miller, Phys. Rev. B **63**, 165109 (2001).

⁸C. S. Lue, J. H. Ross, K. D. D. Rathnayaka, D. G. Naugle, S. Y. Wu, and W.-H. Li, J. Phys.: Condens. Matter **13**, 1585 (2001).

⁹I. Maksimov, D. Baabe, H. H. Klauss, F. J. Litterst, R. Feyerherm, D. M. Tobbens, A. Matsushita, and S. Sullow, J. Phys.: Condens. Matter **13**, 5487 (2001).

¹⁰E. Popiel, M. Tuszynski, W. Zarek, and T. Rendecki, J. Less-Common Met. **146**, 127 (1989); E. Popiel, M. Tuszynski, and W. Zarek, Hyperfine Interact. **51**, 981 (1989).

¹¹T. K. Nielsen, P. Klavin, and R. N. Shelton, Solid State Commun. **121**, 29 (2002).

¹²G. Y. Guo, G. A. Botton, and Y. Nishino, J. Phys.: Condens. Matter **10**, L119 (1998).

¹³R. Weht and W. E. Pickett, Phys. Rev. B **58**, 6855 (1998).

¹⁴A. Bansil, S. Kaprzyk, P. E. Mijnders, and J. Tobola, Phys.

Rev. B **60**, 13396 (1999).

¹⁵D. J. Singh and I. I. Mazin, Phys. Rev. B **57**, 14352 (1998).

¹⁶Ye Feng, M. V. Dobrotvorska, J. W. Anderegg, C. G. Olson, and D. W. Lynch, Phys. Rev. B **63**, 054419 (2001).

¹⁷C. S. Lue, J. H. Ross, C. F. Chang, and H. D. Yang, Phys. Rev. B **60**, R13941 (1999).

¹⁸S. Jemima, Awadhesh Mani, A. Bharathi, Nithya Ravindran, and Y. Hariharan, J. Alloys Compd. **326**, 183 (2001); M. Vasundhara, V. Srinivas, and V. V. Rao, J. Phys.: Condens. Matter **17**, 6025 (2005); C. S. Lue, C. F. Chen, J. Y. Lin, Y. T. Yu, and Y. K. Kuo, Phys. Rev. B **75**, 064204 (2007).

¹⁹Y. Nishino, S. Deguchi, and U. Mizutani, Phys. Rev. B **74**, 115115 (2006).

²⁰Y. Nishino, Mater. Sci. Forum **449-452**, 909 (2004).

²¹K. Endo, H. Matsuda, K. Ooiwa, M. Iijima, T. Goto, K. Sato, and I. Umehara, J. Magn. Magn. Mater. **177-181**, 1437 (1998); H. Matsuda, K. Endo, K. Ooiwa, M. Iijima, Y. Takano, H. Matamura, T. Goto, M. Tokiyama, and J. Arai, J. Phys. Soc. Jpn. **69**, 1004 (2000); T. Kanomata, T. Sasaki, T. Hoshi, T. Narita, T. Harada, H. Nishihara, T. Yoshida, R. Note, K. Koyama, H. Nojiri, T. Kaneko, and M. Motokawa, J. Alloys Compd. **317-318**, 390 (2001).

²²T. Fukuhara, H. Matsuda, S. Masubuchi, K. Ooiwa, Y. Takano, F. Shimizu, and K. Endo, J. Phys. Soc. Jpn. **73**, 13 (2004).

²³A. E. Berkowitz, J. R. Mitchell, M. J. Carey, A. P. Young, S. Zhang, F. E. Spada, F. T. Parker, A. Hutten, and G. Thomas, Phys. Rev. Lett. **68**, 3745 (1992); P. Allia, M. Knobel, P. Tiberto, and F. Vinai, Phys. Rev. B **52**, 15398 (1995).

²⁴M. Rubinstein, V. G. Harris, B. N. Das, and N. C. Koon, Phys. Rev. B **50**, 12550 (1994).

²⁵P. Allia, M. Coisson, J. Moya, V. Selvaggini, P. Tiberto, and F. Vinai, Phys. Rev. B **67**, 174412 (2003).

²⁶M. Vasundhara, Ph.D. thesis, IIT, 2008.

²⁷A. Aharony and E. Pytte, Phys. Rev. Lett. **45**, 1583 (1980).

²⁸E. M. Chudnovsky, W. M. Saslow, and R. A. Serota, Phys. Rev. B **33**, 251 (1986).

- ²⁹J. Q. Xiao, J. S. Jiang, and C. L. Chien, *Phys. Rev. Lett.* **68**, 3749 (1992).
- ³⁰M. El-Hilo, K. O'Grady, and R. W. Chantrell, *J. Appl. Phys.* **76**, 6811 (1994).
- ³¹P. Allia, M. Coisson, G. F. Durin, J. Moya, V. Selvaggini, P. Tiberto, and F. Vinai, *J. Appl. Phys.* **91**, 5936 (2002).
- ³²U. Brück, T. Schneider, M. Acet, and E. F. Wassermann, *Phys. Rev. B* **52**, 3042 (1995).
- ³³Y. Nishino, H. Sumi, and U. Mizutani, *Phys. Rev. B* **71**, 094425 (2005).
- ³⁴S. M. Podgornykh, A. D. Svyazhin, E. I. Shreder, V. V. Marchenkov, and V. P. Dyakina, *J. Exp. Theor. Phys.* **105**, 42 (2007).